KSCE Journal of Civil Engineering (2015) 19(5):1396-1404

DOI 10.1007/s12205-014-0658-0

Structural Engineering

pISSN 1226-7988, eISSN 1976-3808
www.springer.com/12205

The Effects of Cementitious Materials on the Mechanical and Durability Performance of High-Strength Concrete

Joo-Ha Lee* and Young-Soo Yoon**

Received November 4, 2013/Revised April 15, 2014/Accepted July 19, 2014/Published Online December 19, 2014

Abstract

Various tests, focusing on the effects of the type and composition of cementitious materials (ordinary Portland cement, fly ash, slag, low-heat cement, and their combinations) on the mechanical properties and durability of high-strength concrete, were performed to provide experimental data for the application of high-strength concrete to prestressed bridges. Firstly, mix proportions were designed based on a number of trial mixes, taking into account their applicability to prestressed bridges. Mechanical properties, such as compressive strength, modulus of elasticity, splitting tensile strength and flexural strength, were determined. Durability related properties, such as temperature of hydration, resistance to chloride-ion penetration, resistance to freezing-thawing, autogenous and drying shrinkages and creep, were also determined. The effects of cementitious materials on the various properties of high-strength concrete have been demonstrated.

Keywords: *high-strength concretes, admixtures, mechanical properties, concrete durability, prestressing*

1. Introduction

Currently, the demand for High-Strength Concrete (HSC) for a prestressed bridge is gradually increasing as the use of HSC allows engineers to design bridges with longer spans for a given girder cross section and reduces the number of girders per span by increasing the girder spacing, which can lead to substantial costs savings for bridges (Russell, 1994; Hueste *et al.*, 2004). The definition of HSC continues to change as advances in concrete technology make it easier to achieve increasingly higher strength using conventional construction practices. In the late 1970s, 42 MPa was looked upon as being high strength, but more recently 60 MPa has been considered the lower boundary for HSC (FIP-CEB, 1990). The rapid increase in available concrete strength is due principally to the development of superplasticizers and the application of mineral admixtures.

However, design provisions for prestressed concrete members under current codes are primarily based on the empirical relationships of the mechanical properties developed from testing Normal Strength Concrete (NSC) (Hueste *et al.*, 2004). Extrapolation of these empirical equations to materials of higher strength and with different microstructures is unjustified and may be too conservative so that the advantages of using HSC are not fully realized. In addition, there is a lack of experimental data on the relative effects of these cementitious materials on HSC for use in prestressed bridges.

The objective of the study is to obtain information on the mix proportions, mechanical properties and durability of HSC for use in prestressed bridges. Basically, in the mix design, the concrete compressive strength at early age when prestressing forces are introduced to prestressed concrete members, and the slump which is proper for pumping of concrete, were considered to make a concrete suitable for prestressed concrete bridges. In addition to the compressive strength and slump, the air content was considered for enhancement of the durability of prestressed concrete bridges under severe environments. The main parameters investigated were the type and composition of cementitious materials, those being, Ordinary Portland Cement (OPC), Fly Ash (FA), ground granulated Blast furnace Slag (BS) and Low-Heat Cement (LHC). The experimental tests conducted on the mechanical properties included the compressive strength, modulus of elasticity, splitting tensile strength and flexural strength. Tests for the penetration of chloride-ions, freezing-thawing, combined deterioration and temperature of hydration were also performed to investigate the durability of the developed HSC. Furthermore, time-dependent deformations, such as creep, drying and autogenous shrinkage, which are particularly important factors in the design and construction of prestressed concrete bridges, were tested and analyzed.

2. Materials

The cementitious materials used in the tests were OPC, FA, BS

*Member, Assistant Professor, Dept. of Civil Engineering, The University of Suwon, Suwon 445-743, Korea (E-mail: leejooha@suwon.ac.kr)
**Member, Professor, School of Civil, Environmental and Architectural Engineering, Korea University, Seoul 136-701, Korea (Corresponding Author, E-mail: ysyoon@korea.ac.kr)

Table 1. Physical Properties and Chemical Composition of Binders

	OPC	FA	BS	LHC
SiO_2	21.3	52.8	34.3	25.3
Al_2O_3	4.7	22.5	12.7	3.1
Fe_2O_3	3.1	13.4	0.5	3.6
CaO	63.1	4.1	41.3	62.5
MgO	2.9	0.8	5.93	2.0
SO_3	2.2	0.4	2.53	2.3
K_2O	-	0.9	0.5	0.5
Na_2O	-	0.4	0.4	-
Loss on ignition	0.8	3.8	0.48	0.9
C_3S	59.8	-	-	31
C_2S	13.7	-	-	48
C_3A	5.1	-	-	2
C_4AF	9.3	-	-	11
Specific gravity	3.15	2.13	2.91	3.19
Fineness (m^2/kg)	341	348	453	357

and LHC, the chemical compositions and physical properties of which are given in Table 1. The coarse aggregate used was crushed granite, with a specific gravity, fineness modulus and maximum particle size of 2.63, 6.59 and 20 mm, respectively. The fine aggregate was quartz sand with a specific gravity and fineness modulus of 2.59 and 2.84, respectively. The superplasticizer was a polynaphthalene sulfonated-based admixture, with 40% solids in a dark brown solution and a specific gravity of 1.22. A Vinsol resin-type air-entraining admixture was used.

2.1 Mix proportions

For the application of HSC to prestressed bridges, all mixtures were proportioned to give the 28-day design strength of 60 MPa. At the same time, the target 3-day compressive strength of 30 MPa was set up for all mixtures, as the strength of concrete at an early age is considerably significant due to the requirements of the early transfer of prestress. The water to cementitious materials ratio (w/b) was kept at 0.28 for all mixtures. With recent advances in the workability of concrete, the slump is often so large that it is difficult to distinguish different batches. The "slump flow", or the diameter of the base of the slumped material, is often used instead of the height measurement (Saak *et al.*, 2004). Bridge concrete may lose a certain amount of slump due to pumping of the concrete, which is statistically significant (Yazdani *et al.*, 2000). Therefore, the amount of superplasticizer was varied to obtain the desired level of workability maintaining a slump and slump flow of 230 ± 25 and 500 ± 50 mm, respectively. To enable the development of durable concrete for prestressed concrete bridges, the air content of all mixtures was kept at $5.5 \pm 1.0\%$ by adjusting the dosage of the air-entraining admixture.

Based on the type and composition of cementitious material, the mixtures were designated as OPC, FA10, FA20, BS30, BS50, FA15BS35 and LHC. The numbers in the designation represented the percentage mass of the total cementitious materials; for example, Mix FA15BS35 contained 15% fly ash and 35% slag. Mix LHC contained no OPC, but 100% low-heat cement. As shown in Table 2, the mix proportions were determined after a large number of trial mixtures were performed.

3. Experimental Program

After casting, the specimens were covered with plastic sheets, and left in the casting room for 24 hours at 20 ± 2°C, and then demolded and stored in water at 20 ± 3°C until tested.

The concrete hydration temperature was measured on 64 L ($400 \times 400 \times 400$ mm) specimens cast in a semi-adiabatic cube made of Styrofoam. Thermocouples were placed in the center of the specimens and connected to a maturity meter.

The compressive strength and modulus of elasticity were tested on $\phi 100 \times 200$ mm cylinders at 3, 7, 28 and 56 days after casting, according to ASTM C 39 (2011) and ASTM C 469 (2010), respectively. The splitting tensile strength was evaluated using $\phi 100 \times 200$ mm cylinders at 7, 28 and 56 days, according to ASTM C 496 (2011). The flexural strength of prism specimens ($150 \times 150 \times 550$ mm) was determined at 7, 28 and 56 days, according to ASTM C 78 (2010).

The resistance of the concrete to the penetration of chloride ions, measured in terms of the charge passed through the concrete, was determined on 50 mm thick slices of 100 mm diameter cylinders at 28-day. The concrete disc was placed between two solutions, with one end of the disc in contact with a 0.3 N NaOH anolyte solution and the other in contact with a 3% NaCl catholyte solution. After exposure, the concrete disc was split longitudinally, and the depth to which chloride has penetrated into the disc determined by the application of silver nitrate solution to the freshly split surface, which colored the

Table 2. Mix Proportions (kg/m^3)

Mix designation	w/b	Water	Cement	Fly ash	Slag	Fine aggregate	Coarse aggregate
OPC	0.28	170	607	-	-	676	910
FA10	0.28	170	546	61	-	667	898
FA20	0.28	170	486	121	-	658	885
BS30	0.28	170	425	-	182	668	900
BS50	0.28	170	304	-	304	663	892
FA15BS35	0.28	170	304	91	213	653	879
LHC	0.28	170	607*	-	-	676	910

*Low-heat cement

areas containing chloride ions white. The diffusion coefficient was then calculated from Eq. (1):

$$D = \frac{RT}{zFE} \cdot \frac{x_d - \alpha\sqrt{x_d}}{t} \tag{1}$$

$$E = \frac{U-2}{L} \tag{1a}$$

$$\alpha = 2\sqrt{\frac{RT}{zFE}} \cdot erf^{-1}\left(1 - \frac{2c_d}{c_0}\right) \tag{1b}$$

where, c_d = Chloride concentration at which the color changes ($c_d \approx 0.07$ N)
c_0 = Chloride concentration in the catholyte solution ($c_0 \approx 2$ N)
D = Non-steady-state migration coefficient (m^2/sec)
erf = Error function
F = Faraday constant (F = 9.648 × 10^4) (J/V·mol)
L = Thickness of the specimen (m)
R = Gas constant (R = 8.314) (J/K·mol)
t = Test duration (sec)
T = Average value of the initial and final temperatures in the anolyte solution (K)
U = Absolute value of the applied voltage (V)
x_d = Average value of the penetration depths (m)
z = Absolute value of ion valence (for chloride z = 1)

The resistance to freezing and thawing was measured on 100 × 100 × 400 mm concrete prisms, according to ASTM C 666 (2008), Procedure A. To examine how combinations of deicer salt application and freezing-thawing cycles affected deterioration of the concrete, concrete exposed to freeze-thaw cycles in fresh water or in 10% $CaCl_2$ solution was tested. The specimen weight and fundamental transverse frequency were monitored and measured, in accordance with ASTM C 215 (2008), at intervals of 30 cycles.

The autogenous shrinkage was measured on 100 × 100 × 400 mm concrete prisms immediately after casting for periods of up to 28 days by means of an embedded gage. A thermocouple was also inserted into the middle of each specimen to monitor the development of temperature. At an age of 24 hours, the specimens were promptly demolded, and all the surfaces sealed with aluminum adhesive tape. The specimens were then placed vertically in a control room at 23 ± 1°C and 60 ± 3% relative humidity. According to ASTM C 157 (2008), the drying shrinkage was also measured on specimens having the same dimensions, materials and air conditions as those of the specimens used in the autogenous shrinkage test for the same period.

To cope with the difficulties in isolating the strains due to concrete shrinkage from those due to creep, simultaneous creep and concrete shrinkage tests were performed. Strains due to creep were measured on ϕ150 × 300 mm cylinders by means of an embedded gage, according to ASTM C 512 (2010), and concrete shrinkage strains were measured on unloaded specimens having the same dimensions and materials as those loaded. The load was applied at 3-day to find if prestressing forces could be applied to the concrete member at an early age. The creep test was carried out for 90 days.

4. Discussions

4.1 Temperature of Hydration

The temperature of hydration at an early age is shown in Fig. 1. The decrease in the temperature of hydration depends not only on the rate of replacement, but also on the type of cementitious materials incorporated. For example, for FA10, FA20 and BS50, the highest temperature rises were 1.8, 2.7 and 4.9°C lower than that of OPC, respectively. However, the highest temperature rise of BS30 was the same as that of OPC.

It is interesting to note that the adiabatic temperature curve of FA20 seems to have faster hydration temperature development than those of FA10 and OPC. Generally, hydration temperature development becomes faster when the amount of cement increases. In this case, the hydration development could be affected by different dosages of superplasticizer which were used for each mixture to achieve the target slump flow. A high amount of superplasticizer can slow down the hydration process of cement (Nagrockiene *et al*., 2013). Among FA and OPC concretes, the amount of superplasticizer used in OPC was the largest, followed by FA10 and FA20. This seems to affect the time when hydrate reaction start, and FA20 has begun hydration earlier than OPC and FA10. However, OPC has the fastest hydration heat velocity obtained by the slope of the curve, followed by FA10 and FA20. Moreover, the cumulative heat generation was the largest for OPC, and decreased as the amount of FA increased. This observation could be clear when considering the temperature of OPC was a little lower than those of FA10 and FA20 at cast.

As for the ternary mixture, FA15BS35, the highest temperature rise was much lower than that of OPC or the specimens made with single mineral admixtures. LHC had the least temperature rise, which was 12.8°C lower than that of OPC. All specimens had similar arrival times for the highest temperature rise. This phenomenon could be explained by noting the high volume of cementitious materials diluted cement particles at an early age,

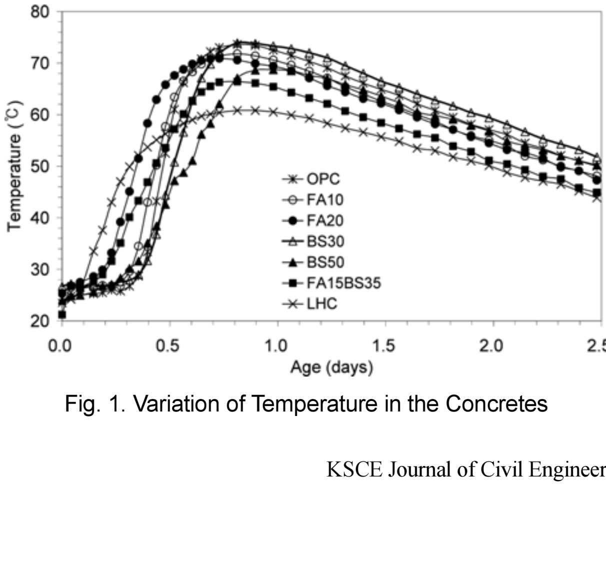

Fig. 1. Variation of Temperature in the Concretes

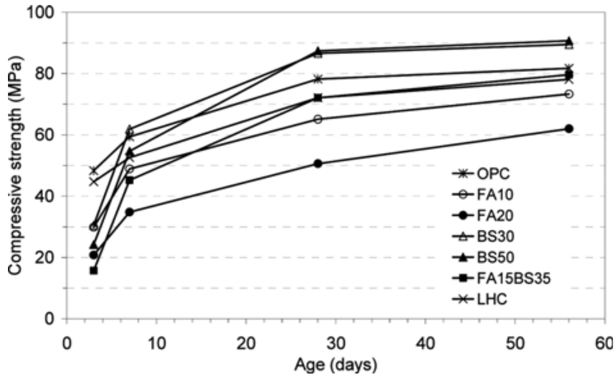

Fig. 2. Development of Compressive Strength

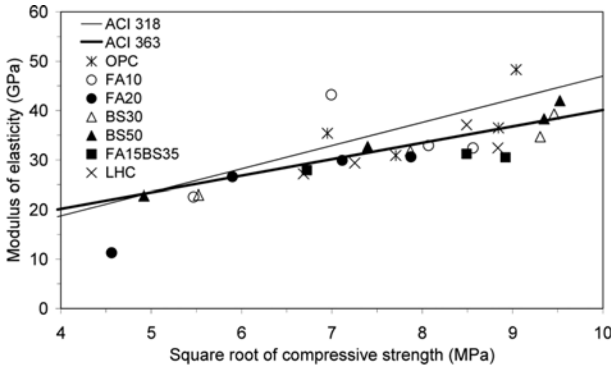

Fig. 3. Comparison of the ACI Equations and Test Results for the Elastic Modulus

resulting in improvement of the hydration environment of the cement. As a result, for HSC with a low w/b, the cement hydration process was accelerated.

4.2 Compressive Strength

The strengths developed by the concretes at 3, 7, 28 and 56 days are shown in Fig. 2. As expected, the replacement of cement by the weight of mineral admixtures resulted in decreased compressive strengths at an early age compared with the strength of OPC and LHC. Especially, for the concretes having a large proportion of mineral admixture, such as FA20, BS50 and FA15BS35, the target strength value of 30 MPa at 3-day was not achieved. At 7-day; however, the compressive strengths of all the concretes exceeded 30 MPa, and the 28-day design strength of 60 MPa was achieved for all mixes, with the exception of FA20. The addition of fly ash caused a considerable reduction in the compressive strength, which was reduced by as much as 35% on the addition of 20% fly ash at 28-days. Because of the slow pozzolanic reactions of fly ash, continuous wet curing and favorable curing temperatures are required for the proper development of strength. It should be noted that fly ash has been used in the production of HSC when cured for a long period of time (Toutanji *et al*., 2004). Although concretes incorporating fly ash, such as FA10, FA20 and FA15BS35, developed lower strengths than OPC, their rate of strength increase after 28 days was higher than the other concretes. Concretes incorporating slag, such as BS30 and BS50, had the highest strengths at 28 and 56 days.

4.3 Modulus of Elasticity

The moduli of elasticity of the concretes determined at 3, 7, 28 and 56 days are shown in Table 3. To evaluate the accuracy of equations; ACI 318-11 (2011) and ACI 363R-10 (2010), in predicting the modulus of elasticity when supplementary cementitious materials are added to the concrete, the modulus of elasticity from the test results was compared with those obtained using these equations, as shown in Fig. 3. The prediction equations, ACI 318-11 (2011) and ACI 363R-10 (2010), are given by Eqs. (2) and (3), respectively:

$$E_c = 4700\sqrt{f_c'} \text{ (MPa)} \tag{2}$$

$$E_c = 3320\sqrt{f_c'} + 6900 \text{ (MPa) for } 21 \text{ MPa} \le f_c' \le 83 \text{ MPa} \tag{3}$$

where, f_c' is the specified compressive strength of concrete in MPa.

As shown in Fig. 3, ACI 363R-10 (2010) has a better prediction modulus values than ACI 318-11 (2011). This graph shows that the prediction equation of ACI 363R-10 (2010) can be used to predict the modulus values for HSC incorporating supplementary cementitious materials.

The initial modulus of elasticity is important to the precast prestressed industry for investigating certain effects, such as elastic shortening (Mokhtarzadeh *et al*., 1995). The results

Table 3. Modulus of Elasticity, Splitting Tensile and Flexural Strength Test Results

Mix designation	Modulus of elasticity (GPa)				Splitting tensile strength (MPa)			Flexural strength (MPa)		
	3-day	7-day	28-day	56-day	7-day	28-day	56-day	7-day	28-day	56-day
OPC	35.4	30.9	36.5	48.3	3.6	3.9	3.7	9.8	11.1	10.1
FA10	22.6	43.2	32.9	32.4	3.2	3.5	4.0	8.4	10.4	9.3
FA20	11.3	26.6	29.9	30.6	3.3	3.4	3.2	8.3	8.3	10.3
BS30	23.0	31.8	34.7	39.3	3.0	3.6	3.5	12.5	12.1	11.1
BS50	22.8	32.7	38.3	42.0	3.9	4.4	4.5	11.1	10.2	11.5
FA15BS35	10.7	27.9	31.2	30.5	3.9	4.2	5.7	8.3	10.6	10.5
LHC	27.2	29.7	37.1	32.4	3.3	3.9	4.5	6.9	9.2	9.2

obtained from this study indicate that the 3-day modulus of elasticity measured on concretes incorporating mineral admixtures was less than 70% of that obtained at 28-days, while those of OPC and LHC were approximately 97 and 73.3% of their 28-day values, respectively. At 7-days, however, the elastic moduli of all types of concrete were over 80% of those obtained at 28-days.

4.4 Splitting Tensile and Flexural Strengths

Table 3 shows the test results of the splitting tensile and flexural strengths. The tensile to compressive strength ratio of concrete depends on the general level of the compressive strength; the higher the compressive strength, the lower the ratio. The direct tensile to compressive strength ratio for NSC is reported to be between 8~9%, but that for HSC is decreased to be about 5% (Mehta and Monteiro, 1993; Neville, 1995). The test results show that the splitting tensile to compressive strength ratio of all the concretes ranged from 3.9 to 9.5%, and the flexural strength was found to increase with increasing compressive strength. However, the type and composition of cementitious material showed no significant effects on the splitting tensile and flexural strengths.

4.5 Resistance to Chloride-ion Penetration

The results for the resistance of the concrete to chloride-ion penetration are given in Fig. 4. The effect of cement replacement on the resistance to chloride-ion penetration is clearly illustrated. As the rate of replacement increases, the chloride migration coefficient decreases, as both fly ash and blast furnace slag may improve the pore size distribution as well as the pore shape of concrete. FA15BS35 showed the lowest chloride-ion permeability of all the concretes tested. However, FA20 had the highest chloride migration coefficient which was more than two times larger compared to OPC. This is inconsistent with the other results from the literature (Leng *et al*., 2000). At the test age, FA20 had the lowest compressive strength, that is, more pores and diffusing paths may form with the low strength, so the chloride ion diffusion coefficient may increase. In addition, based on some researches reporting on the relationship between concrete compressive strength and chloride resistance, the chloride migration coefficients can differ by more than two times when concrete compressive strengths differ by about 200% (Al-Amoudi *et al*., 2009; Lee and Kwon, 2012; Ramezanianpour *et al*., 2011; Yoon *et al*., 2005).

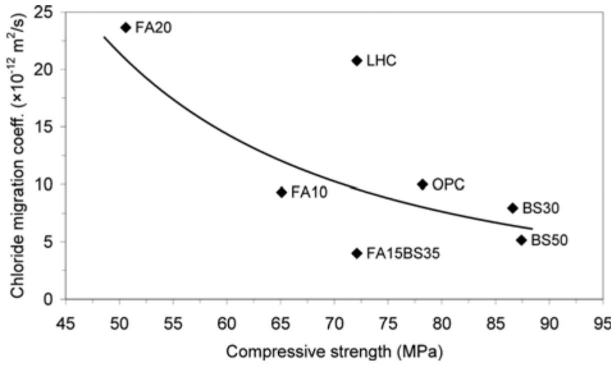

Fig. 5. Relation between the Chloride Migration Coefficient and Compressive Strength

Figure 5 shows the relation between the chloride migration coefficient and compressive strength. The chloride migration coefficient decreased with increasing compressive strength, but this was not the case for LHC. Yoo *et al.* (2007) indicated that LHC has a lower chloride migration coefficient than OPC for similar compressive strengths. According to their results, the chloride migration coefficients of OPC and LHC were 9.1×10^{-12} m^2/s and 15.7×10^{-12} m^2/s, respectively when their compressive strengths were about 60MPa. These phenomena may be related to the relatively low compressive strength and slow hydration rate. Further research is needed to clarify this possible link.

4.6 Resistance to Freezing and Thawing

The durability factors of the test specimens in water and $CaCl_2$ solution are plotted in Fig. 6. Due to the limits of the chamber capacity for storage, BS30 was excluded from the test as other studies have shown no correlation between the slag contents and the durability factor (Toutanji *et al*., 2004). For all specimens immersed in fresh water, with the exception of FA20, the calculated durability factors were over 90 after 300 cycles. As observed from the results, the greater the amount of fly ash, the

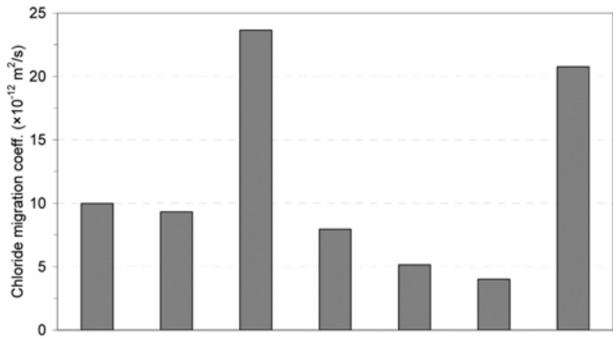

Fig. 4. Chloride Migration Coefficient of the Concretes

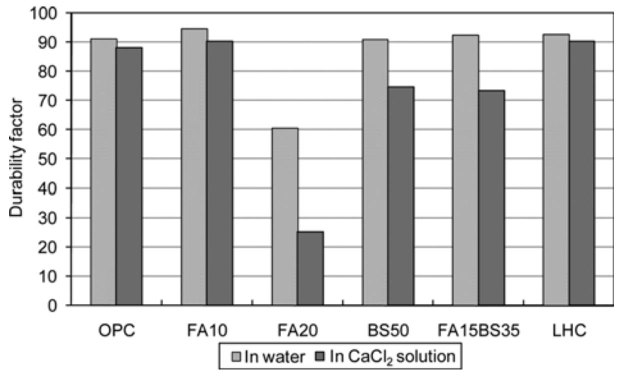

Fig. 6. Durability Factor of the Concretes in Water and $CaCl_2$ Solution

lower the resistance to freeze and thaw exposure. Considering the slow pozzolanic reactions of fly ash, a curing period of only 14 days may result in decreased resistance to freezing and thawing.

In actual concrete applications, the concrete surface scales markedly when exposed to freeze–thaw cycles and de-icing salt (Mu *et al.*, 2002). The results shown in Fig. 6 indicate that concretes subjected to freeze–thaw cycles in $CaCl_2$ solution had lower durability factors than in water, with the test results for the concretes in $CaCl_2$ solution showing similar tendencies to those in water. However, for the mixes with low or no replacement rates, such as FA10, OPC and LHC, the chloride solution did not significantly affect the resistance to freezing and thawing.

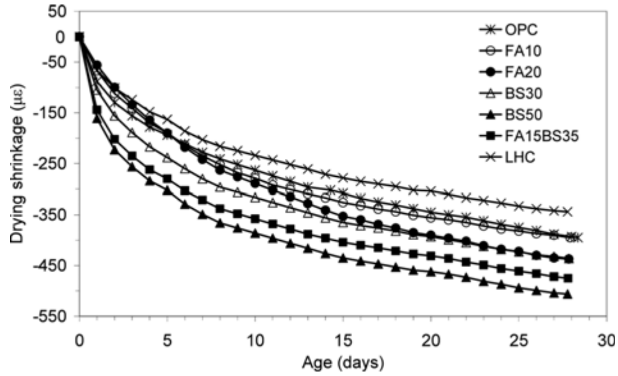

Fig. 8. Drying Shrinkage

4.7 Autogenous and Drying Shrinkage

Although there were no differences between the autogenous and drying shrinkages in relation to decreased humidity in the hardened cement body, there is a difference in their mechanisms; drying shrinkage is the evaporation of water towards the outer environments; whereas, autogenous shrinkage is the consumption of water due to a hydration reaction (JCI, 1999). Therefore, the small amount of water used for mixing in HSC is rapidly consumed by early age hydration of the cement. This is the main reason why a large amount of autogenous shrinkage is observed with HSC. Besides w/c and cement content, various pozzolanic materials also affect the autogenous shrinkage behavior of HSC in different manners (Tazawa and Miyazawa, 1995).

It is well known that the inclusions of fly ash and blast-furnace slag result in significant decrease and increase of autogenous shrinkage of HSC, respectively (Jiang *et al.*, 2014; Lim and Wee, 2000; Neville, 1995; Tazawa and Miyazawa, 1995). In that sense, test results of autogenous shrinkage from the current study are consistent with those from the previous other researches. Figs. 7 and 8 show the results of the autogenous and drying shrinkage tests, and it is evident that the autogenous shrinkage increases when part of the OPC is replaced by slag. The higher autogenous shrinkage of concrete containing slag than that of OPC seems to be due to the greater chemical shrinkage which leads to faster and greater self-desiccation, and results in larger autogenous shrinkage (Jiang *et al.*, 2014). With further increases

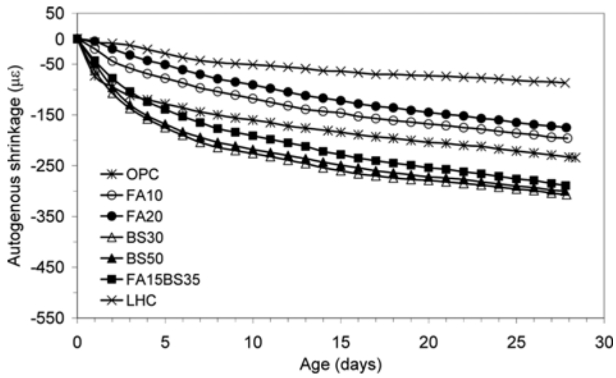

Fig. 7. Autogenous Shrinkage

in the slag content, however, the autogenous shrinkage slightly decreases. Lim and Wee (2000) reported a similar trend that the autogenous shrinkage increased up to the certain replacement percentage of slag and then decreased as the replacement level increased. In this case the low autogenous shrinkage may be due to a lower degree of self-desiccation as a large amount of slower hydrating slag results in small amounts of OPC and water limiting the production of calcium hydroxide that is needed to activate the pozzolanic reaction of slag (Lim and Wee, 2000). The effect of slag on increasing the autogenous shrinkage was also observed in drying shrinkage, as shown in Fig. 8. However, contrary to the effect of the replacement rate of slag on autogenous shrinkage, the dry shrinkage increases considerably with increasing slag content.

The incorporation of fly ash into HSC leads to a decrease in autogenous shrinkage; the higher the fly ash content, the lower the autogenous shrinkage. The reason why the autogenous shrinkage of concrete containing fly ash is smaller than that of OPC concrete can be explained by hydration characteristic of the pozzolanic material. With the substitution of cement by fly ash, internal relative humidity of concrete decreases relatively slowly, self-desiccation may not practically occurs, and consequently reduces autogenous shrinkage (Jiang *et al*., 2014). Contrary to the test results of autogenous shrinkage in Fig. 7, the drying shrinkage of concrete containing fly ash increased as the replacement percentage of fly ash increased, as shown in Fig. 8. This result is in good agreement with various researches (Kayali *et al.*, 1999; Mehta and Monteiro, 1993; Ravindrarajah and Tam, 1989). Mehta and Monteiro (1993) indicated that concretes containing pozzolans like fly ash increasing the volume of fine pores show higher drying shrinkage because drying shrinkage is directly associated with the water held by small pores in the size range 3 to 20 nm. Another reason for the increase in the drying shrinkage of concrete containing fly ash is the increased water to cement ratio by the substitution of cement by fly ash whose pozzolanic reaction doesn't cause water reduction.

However, fly ash, as with slag, helps increase drying shrinkage, as shown by Fig. 8. When both slag and fly ash are incorporated, the effect of the slag appears to dominate the shrinkage characteristic of HSC. The trend for FA15BS35 was similar in

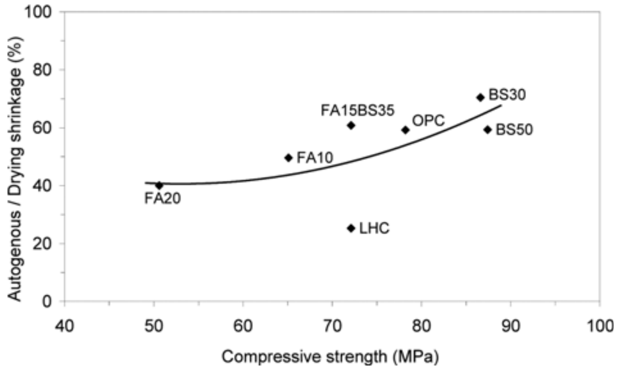

Fig. 9. Relation between the Autogenous Shrinkage and Compressive Strength

terms of both autogenous and dry shrinkages to that of concretes incorporating slag. LHC showed the least autogenous and dry shrinkages. In addition, LHC had a very low ratio of autogenous shrinkage to drying shrinkage, which was only 25.3%. The relation between the autogenous to drying shrinkage ratio at 28-days and compressive strength is given in Fig. 9. The autogenous to drying shrinkage ratio increased with increasing compressive strength, suggesting most of the drying shrinkage can not be attributed to evaporation, but to autogenous shrinkage for HSC.

4.8 Creep

The specific creep data (strain due to creep per unit stress that cylinders are subjected to) up to 90 days are shown in Fig. 10. BS30 was not tested due to the number limits of the loading device. According to previous research, concrete with a less slag content in its binder gives lower specific creep (Khatri *et al.*, 1995). Although both slag and fly ash were incorporated with FA15BS35, when FA15BS35 and BS50 were compared, they showed the same tendency as the previous research, as observed in Fig. 10. At an early age, the specific creep of concretes incorporating slag, such as BS50 and FA15BS35, was lower than that of OPC. In the long term; however, their specific creep was higher than that of OPC. Especially, BS50 had the second highest specific creep, following LHC, and the specific creep of BS50 and LHC trended upward, even at 90 days. The concretes

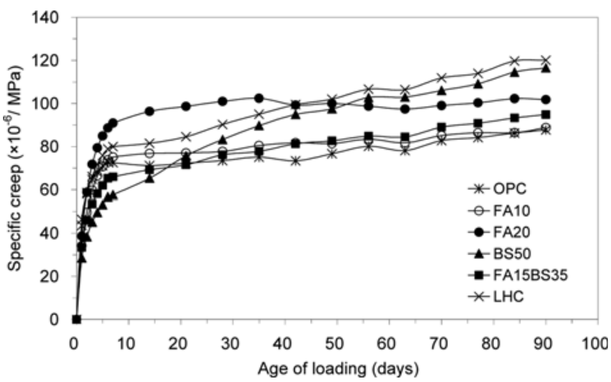

Fig. 10. Specific Creep of the Concretes

incorporating fly ash showed higher specific creep than that of OPC. In addition, when FA10 and FA20 were compared, it appears that concrete with higher fly ash content gave higher specific creep, but this was inconsistent with other reports from the literatures (Khatri *et al.*, 1995; Sivasundaram *et al.*, 1991). This phenomenon can be explained by noting that the age at the time of loading was 3-days. At this age, fly ash concrete has relatively low compressive strength due to its slow pozzolanic reactions. Indeed, as shown in Fig. 10, the specific creep of FA10 and FA20 increased markedly during the first 7 days, but thereafter, increased more slowly than any other of the concretes.

5. Conclusions

To provide information on the mix proportions, mechanical properties and durability of HSC for use in prestressed bridges, this research mainly focused on studying the effects of the type and composition of cementitious materials on the properties of HSC. Firstly, mix proportions were designed based on a number of trial mixes, taking into account the early age compressive strength, workability and air content so that the developed concrete would be suitable for prestressed bridges. Based on the results of this research, the following conclusions were drawn:

1. For the ternary mixture of FA15BS35 and LHC, the highest temperature rise was much lower than that of OPC. All specimens were at similar levels for the time when the highest temperature rise was achieved.
2. Supplementary cementitious materials resulted in decreased compressive strengths at early ages. At 28 and 56 days; however, the concretes incorporating slag had higher strengths than OPC. The rate of strength increase of fly ash concrete after 28 days was the highest.
3. The ACI 363R-10 (2010) equation seems to provide a good prediction of the elastic modulus of HSC incorporating supplementary cementitious materials. At early ages, the percentage gain in the elastic modulus of concretes incorporating the mineral admixtures was lower than those of OPC and LHC.
4. The higher the compressive strength, the lower the tensile to compressive strength ratio. The flexural strength was found to increase with increasing compressive strength. The type and composition of cementitious material had no significant effects on the splitting tensile and flexural strengths.
5. Regardless of the type of mineral admixtures, the chloride-ion permeability was improved with increasing rate of replacement. In general, the chloride migration coefficient decreased with increasing compressive strength. However, LHC showed inferior resistance to chloride-ions, although its compressive strength was relatively high.
6. In general, and regardless of the type of mineral admixtures and the replacement percentage, not only concretes incorporating supplementary cementitious materials, but also OPC and LHC, had excellent durability factors to repeated cycles of freezing and thawing. Concretes subjected to freeze–thaw

cycles in CaCl2 solution had lower durability factors than in water, but the chloride solution did not significantly affect the resistance to freezing and thawing of concretes with low or no replacement rates.

7. The increase in the incorporation of slag leads to increases in both the autogenous and drying shrinkages of HSC. The incorporation of fly ash decreases the autogenous shrinkage, but increases the drying shrinkage in the same manner as the incorporation of slag. When both slag and fly ash are incorporated, the effect of the slag appears to dominate the shrinkage characteristic of HSC. The shrinkage characteristic of LHC is superior to that of OPC. Most of the drying shrinkage is attributed to the autogenous shrinkage for HSC.
8. Concretes incorporating supplementary cementitious materials showed higher specific creep than that of OPC. When a load is applied at an early age, the specific creep of fly ash concrete increases markedly at an early age, but thereafter, increases very slowly. LHC had the highest specific creep.

Notations

The following symbols are used in this paper:

c_d = Chloride concentration at which the color changes, N
c_0 = Chloride concentration in the catholyte solution, N
D = Non-steady-state migration coefficient, m^2/sec
erf = Error function
F = Faraday constant, J/V·mol
f_c' = Specified compressive strength of concrete, MPa
L = Thickness of the specimen, m
R = Gas constant, J/K·mol
T = Average value of the initial and final temperatures in the anolyte solution, K
t = Test duration, sec
U = Absolute value of the applied voltage, V
x_d = Average value of the penetration depths, m
z = Absolute value of ion valence

Acknowledgements

This research was supported by Basic Science Research Program through the National Research Foundation of Korea (NRF) funded by the Ministry of Science, ICT & Future Planning (grant number = 2013R1A1A1005577).

References

ACI Committee 318 (2011). *Building code requirements for structural concrete (ACI 318-11) and commentary (318R-11)*, American Concrete Institute, Farmington Hill, Mich.

ACI Committee 363 (2010). *Report on high-strength concrete (ACI 363R-10)*, American Concrete Institute, Farmington Hills, Mich.

Al-Amoudia, O. S. B., Al-Kuttia, W. A., Ahmada, S., and Maslehuddin, M. (2009). "Correlation between compressive strength and certain durability indices of plain and blended cement concretes." *Cement and Concrete Composites*, Elsevier, Vol. 31, No. 9, pp. 672-676, DOI: 10.1016/j.cemconcomp.2009.05.005.

ASTM C157 (2008). *Standard test method for length change of hardened hydraulic-cement mortar and concrete*, ASTM International, West Conshohocken, PA.

ASTM C215 (2008). *Standard test method for fundamental transverse, longitudinal, and torsional frequencies of concrete specimens*, ASTM International, West Conshohocken, PA.

ASTM C39 (2011). *Standard test method for compressive strength of cylindrical concrete specimens*, ASTM International, West Conshohocken, PA.

ASTM C469 (2010). *Standard test method for static modulus of elasticity and Poisson's ratio of concrete in compression*, ASTM International, West Conshohocken, PA.

ASTM C496 (2011). *Standard test method for splitting tensile strength of cylindrical concrete specimens*, ASTM International, West Conshohocken, PA.

ASTM C512 (2010). *Standard test method for creep of concrete in compression*, ASTM International, West Conshohocken, PA.

ASTM C666 (2008). *Standard test method for resistance of concrete to rapid freezing and thawing*, ASTM International, West Conshohocken, PA.

ASTM C78 (2010). *Standard test method for flexural strength of concrete (using simple beam with third-point loading)*, ASTM International, West Conshohocken, PA.

FIP-CEB Working Group on High Strength Concrete (1990). *High strength concrete: State-of-the-art report*, CEB bulletin d'Information No. 197, FIP-CEB, London.

Hueste, M. B. D., Chompreda, P., Trejo, D., Cline, D. B. H., and Keating, P. B. (2004). "Mechanical properties of high-strength concrete for prestressed members." *ACI Structural Journal, American Concrete Institute*, Vol. 101, No. 4, pp. 457-465, DOI: 10.14359/13331.

Japan Concrete Institute(JCI) Technical Committee on Autogenous Shrinkage of Concrete (1999). *Committee report-autogenous shrinkage of concrete*, E & FN Spon, London and New York.

Jiang, C., Yang, Y., Wang, Y., Zhou, Y., and Ma, C. (2014). "Autogenous shrinkage of high performance concrete containing mineral admixtures under different curing temperatures." *Construction and Building Materials*, Elsevier, Vol. 61, pp. 260-269, DOI: 10.1016/j.conbuildmat.2014.03.023.

Kayalia, O., Haque, M. N., and Zhu, B. (1999). "Drying shrinkage of fibre-reinforced lightweight aggregate concrete containing fly ash." *Cement and Concrete Research*, Elsevier, Vol. 29, No. 11, pp. 1835-1840, DOI: 10.1016/S0008-8846(99)00179-9.

Khatri, R. P., Sirivivatnanon, V., and Gross, W. (1995). "Effect of different supplementary cementitious materials on mechanical properties of high performance concrete." *Cement and Concrete Research*, Elsevier, Vol. 25, No. 1, pp. 209-220, DOI: 10.1016/0008-8846(94)00128-L.

Lee, S. H. and Kwon, S. J. (2012). "Experimental study on the relationship between time-dependent chloride diffusion coefficient and compressive strength." *Journal of the Korea Concrete Institute,* Korea Concrete Institute, Vol. 24, No. 6, pp. 715-726, DOI: 10.4334/JKCI.2012.24.6.715. (in Korean).

Leng, F., Feng, N., and Lu, X. (2000). "An experimental study on the properties of resistance to diffusion of chloride ions of fly ash and blast furnace slag concrete." *Cement and Concrete Research*, Elsevier, Vol. 30, No. 6, pp. 989-992, DOI: 10.1016-S0008-8846(00)00250-7.

Lim, S. N. and Wee, T. H. (2000). "Autogenous shrinkage of ground-granulated blast-furnace slag concrete." *ACI Materials Journal,* American Concrete Institute, Vol. 97, No. 5, pp. 587-593, DOI: 10.14359/9291.

Mehta, P. K. and Monteiro, P. J. M. (1993). *Concrete: Structure, properties, and materials, 2nd ed.*, Prentice-Hall, New Jersey.

Mokhtarzadeh, A., Kriesel, R., French, C., and Snyder, M. (1995). "Mechanical properties and durability of high-strength concrete for prestressed bridge girders." *Transportation Research Record,* Transportation Research Board, Issue 1478, pp. 20-29.

Mu, R., Miao, C., Luo, X., and Sun, W. (2002). "Combined deterioration of concrete subjected to loading, freeze-thaw cycles and chloride salt attack." *Magazine of Concrete Research,* ICE Publishing, Vol. 54, No. 3, pp. 175-180, DOI: 10.1680/macr.2002.54.3.175.

Nagrockiene, D., Pundiene, I., and Kicaite, A. (2013). "The effect of cement type and plasticizer addition on concrete properties." *Construction and Building Materials*, Elsevier, Vol. 45, pp. 324-331, DOI: 10.1016/j.conbuildmat.2013.03.076.

Neville, A. M. (1995). *Properties of concrete, 4th ed.*, Longman Group Ltd., London.

Ramezanianpour, A. A., Pilvar, A., Mahdikhani, M., and Moodi, F. (2011). "Practical evaluation of relationship between concrete resistivity, water penetration, rapid chloride penetration and compressive strength." *Construction and Building Materials*, Elsevier, Vol. 25, No. 5, pp. 2472-2479, DOI: 10.1016/j.conbuildmat.2010.11.069.

Ravindrarajah, R. S. and Tam, C. T. (1989). "Properties of concrete containing low-calcium fly ash under hot and humid climate." *ACI Special Publication, American Concrete Institute*, Vol. 114, pp. 139-156, DOI: 10.14359/1894.

Russell, B. W. (1994). "Impact of high-strength concrete on the design and construction of pretensioned girder bridges." *PCI Journal,* Precast/Prestressed Concrete Institute, Vol. 39, No. 4, pp. 76-89.

Saak, A. W., Jennings, H. M., and Shah, S. P. (2004). "A generalized approach for the determination of yield stress by slump and slump flow." *Cement and Concrete Research*, Elsevier, Vol. 34, No. 3, pp. 363-371, DOI: 10.1016/j.cemconres.2003.08.005.

Sivasundaram, V., Carette, G. G., and Malhotra, V. M. (1991). "Mechanical properties, creep, and resistance to diffusion of chloride ions of concretes incorporating high volumes of ASTM Class F fly ashes from seven different sources." *ACI Materials Journal,* American Concrete Institute, Vol. 88, No. 4, pp. 407-416, DOI: 10.14359/1930.

Tazawa, E. and Miyazawa, S. (1995). "Influence of cement and admixture on autogenous shrinkage of cement paste." *Cement and Concrete Research*, Elsevier, Vol. 25, No. 2, pp. 281-287, DOI: 10.1016/0008-8846(95)00010-0.

Toutanji, H., Delatte, N., Aggoun, S., Duval, R., and Danson, A. (2004). "Effect of supplementary cementitious materials on the compressive strength and durability of short-term cured concrete." *Cement and Concrete Research*, Elsevier, Vol. 34, No. 2, pp. 311-319, DOI: 10.1016/j.cemconres.2003.08.017.

Yazdani, N., Bergin, M., and Majtaba, G. (2000). "Effect of pumping on properties of bridge concrete." *Journal of Materials in Civil Engineering,* American Society of Civil Engineers, Vol. 12, No. 3, pp. 212-219, DOI: 10.1061/(ASCE)0899-1561(2000)12:3(212).

Yoo, J. K., Park, S. J., and Oh, B. H. (2007). "Effects of cement and mineral admixture on migration of chloride ions and generation of hydration heat in concrete." *Daewoo Construction Technology Report,* Daewoo Engineering & Construction Co. Ltd., Vol. 29, pp. 106-115.

Yoon, E. S., Lee, T. W., and Park, S. B. (2005). "Analysis of correlation between compressive strength, void ratio and chloride diffusion coefficient of concrete using various kinds of cement." *Journal of the Korea Concrete Institute*, Korea Concrete Institute, Vol. 17, No. 5, pp. 735-742 (in Korean).